

Ferrotoroidic polarons in antiferrodistortive SrTiO₃Takahiro Shimada ^{1,*}, Yuuki Ichiki,¹ Gen Fujimoto,¹ Le Van Lich ², Tao Xu,³ Jie Wang,⁴ and Hiroyuki Hirakata ¹¹*Department of Mechanical Engineering and Science, Kyoto University, Nishikyo-ku, Kyoto 615–8540, Japan*²*School of Materials Science and Engineering, Hanoi University of Science and Technology, No. 1, Dai Co Viet Street, Hanoi, Vietnam*³*Materials Genome Institute, Shanghai University, Shanghai Materials Genome Institute, Shanghai 200444, China*⁴*Department of Engineering Mechanics & Key Laboratory of Soft Machines and Smart Devices of Zhejiang Province, School of Aeronautics and Astronautics, Zhejiang University, Hangzhou 310027, China*

(Received 6 February 2020; revised manuscript received 27 April 2020; accepted 28 April 2020; published 1 June 2020)

Ultrascale ferroelectrics with nontrivial topological field textures such as polar vortices, skyrmions, and merons hold promise in technological paradigms. Such nontrivial ferroic orders and their functionalities, however, inevitably disappear below a critical size of several nanometers. Here, we propose a strategy to overcome this limitation and design atomically small ferroelectrics with topological polarization vortices by engineering excess-electron polarons. Our first-principles calculations demonstrate that excess-electron polarons formed in antiferrodistortive SrTiO₃ induce localized ferroelectric polarization with a topological vortex form due to local symmetry breaking and demonstrate the possibility of an atomic-scale “ferrotoroidic” materials. We further show that the electron polaron carries a magnetic moment coupled with ferrotoroidicity, i.e., the magnetoelectric effect. We also discuss possible methods to switch the toroidal moment via the magnetoelectric effect. Our result, thus, provides insight into the ultimate miniaturization of ferrotoroidic materials and a class of functional polaron families.

DOI: [10.1103/PhysRevB.101.214101](https://doi.org/10.1103/PhysRevB.101.214101)**I. INTRODUCTION**

Ferroelectric perovskite oxides, such as BaTiO₃ and PbTiO₃, have lately attracted tremendous attention owing to their distinguished dielectric, ferroelectric, and electromechanical properties and technological applications such as in ferroelectric memories, sensors, microelectromechanical systems (MEMS), actuators, etc. [1–3]. In recent years, nanoscale ferroelectrics such as nanothinfilms [4], nanowires [5], and nanotubes [6] have been synthesized with advances in manufacturing technology. In these nanoferroelectrics, the polarization effect is different from that of macro counterparts because the influence of the depolarization field accompanying the surface charge is applied to the entire material [7–9]. Vortex polarization is one of the well-known examples for nontrivial topological polarization patterns that emerge in nanoferroelectrics. Vortex polarization is known to generate an order variable called the toroidal moment due to the nature of a vortex while the polarization of the points mutually cancels out when the polarizations are summed up [10–12]. Importantly, the toroidal moment can be reversed according to the rotational direction of the vortex polarization (ferrotoroidicity). Hence, the vortex polarization is expected to find applications in ultra-large-capacity memories that store information [10]. To increase the speed and capacity of integrated devices such as memories, it is necessary to integrate the components at high density. Therefore, miniaturization of vortex polarization and ferrotoroidic materials is required. However, in ferroelectrics, the ferroelectricity

disappears when the size of the material is lower than a critical threshold. For example, ferroelectric PZT and BaTiO₃ nanodots are reported to lose their ferroelectricity when their size drops below 3 to 5 nm [10,13]. Therefore, there is a physical size limit to the miniaturization of ferroelectric materials via material processing in principle and a strategy is required for further miniaturization of vortex polarization.

Excess electrons or holes often exist in oxide materials due to the method of injecting electrons from the electrode in which high voltage is applied to the insulator, or the compositional mismatch derived from lattice defects such as vacancies, dislocations, and grain boundaries [14–16]. Excess electrons or holes in the material are known to form a free-carrier state uniformly distributed throughout the material or a polaronic state localized at one atomic site in the material with a local lattice distortion [14]. Due to strong electron-phonon interaction at the polaronic site, local mismatch in charge balance occurs and atoms around the polaron are displaced, leading to the formation of characteristic atomic and electronic structures at the local polaronic site. As a result, the crystal symmetry breaking due to the formation of polarons induces ionic displacement in oxide materials, giving rise to local dipole moments and polarizations. So far, we have attempted to design physical properties via the local symmetry breaking from lattice defects in crystals instead of polarons, such as ferroelectricity and magnetism via lattice defects such as vacancies [17], dislocations [18], and grain boundaries [19] to create ferroelectric and multiferroic materials smaller than the critical size. However, there has not yet been an example of creating atomic scale ferrotoroidic materials with vortex polarizations.

*shimada@me.kyoto-u.ac.jp

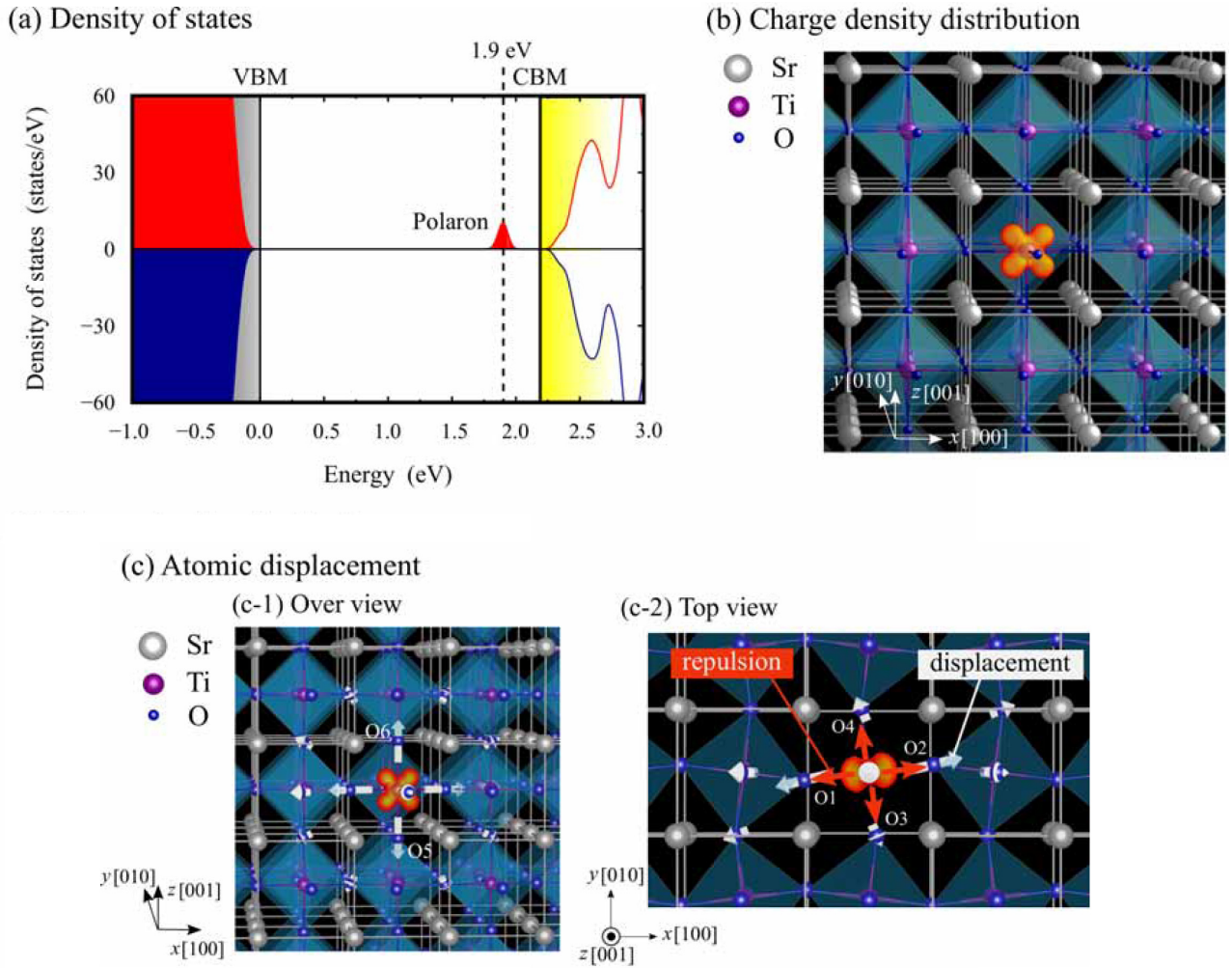


FIG. 1. (a) Electronic density of states (DOS) of the excess-electron polaron in SrTiO₃. The red and blue areas (lines) indicate the occupied (unoccupied) states of up- and down-spins, respectively. The mid-gap state is the Ti d_{xz} state occupied by the one excess electron. (b) Charge density distribution of the polaronic state in SrTiO₃. The orange area represents the isosurface of charge density of $0.01e/\text{\AA}^3$. White arrows indicate the displacements of O atoms around the polaron. (c) Atomic displacement d (white arrows) around the polaron in SrTiO₃.

In this study, we demonstrate that the excess-electron polaron formed in antiferrodistortive (AFD) SrTiO₃ induces localized ferroelectric polarization with a topological vortex form using first-principles calculations and also demonstrate the possibility of an atomic-scale “ferrotoroidic” material. Further, we demonstrate that electron polarons carry magnetic moments coupled with ferrotoroidicity, i.e., the magnetoelectric effect. Finally, we discuss possible methods to switch the toroidal moment.

II. SIMULATION MODELS AND PROCEDURE

First-principles density functional theory (DFT) [20,21] calculations were performed using the VASP [22,23] code. The projector-augmented wave pseudopotential method [24,25] was employed and the electrons of $4s$, $4p$, and $5s$ electrons for Sr, the $3s$, $3p$, $3d$, and $4s$ electrons for Ti, and the $2s$ and $2p$ electrons for O were treated as valence electrons. The electronic wave function was expressed using a plane wave basis set, and the cutoff energy of the plane wave was set to 400 eV. The simulation supercell model consisted of $4 \times 4 \times 4$ unit

cells of AFD SrTiO₃. The $3 \times 3 \times 3$ Monkhorst-Pack [26] k -point mesh was used for the Brillouin zone integration. The system was charged to negative due to introduction of an excess electron with homogeneous background charge condition to satisfy the electrical neutrality condition [27]. To correctly describe the polaronic state of excess electron in SrTiO₃, we used the DFT+ U method for the generalized correlation of the correlation term with Perdew-Bruke-Ernzerhof *et al.* [28]. The values $U = 4.96$ eV and $J = 0.51$ eV, calculated using the first-principles approximation, based on the constrained random phase approximation method, were applied to the $3d$ orbital of the Ti atom [29]. It has been reported that localized electronic states in SrTiO₃ can be well reproduced by these U and J values [29]. See the Supplemental Material for more details [30].

III. RESULTS AND DISCUSSION

A. Formation of the excess-electron polaron

Figure 1(a) depicts the electronic density of states (DOS) of the excess-electron-doped SrTiO₃. Within the band gap,

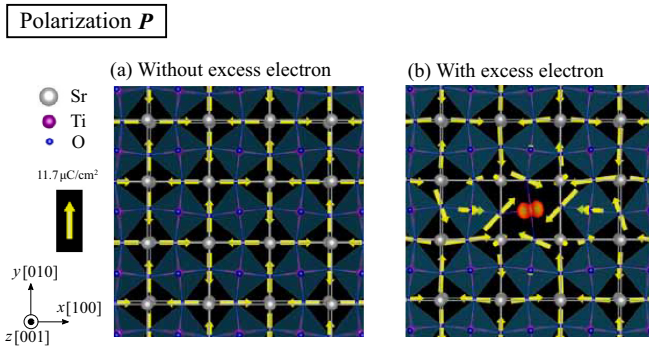


FIG. 2. The distribution of polarization \mathbf{P} in SrTiO₃ (a) without polaron and (b) with polaron. The yellow arrows indicate local polarization. The orange area represents the iso-surface of polaron charge densities of $0.01e/\text{\AA}^3$. The local polarization of $11.7\mu\text{C}/\text{cm}^2$ in undoped AFD SrTiO₃ is shown as reference in the left panel.

an electronic state exists at an energy level of 1.9 eV higher than the valence band maximum, as represented by the black dotted line. This state does not exist in undoped SrTiO₃, and thereby, the energy level appearing in the band gap can thus be attributed to the excess electron. Figure 1(b) depicts the charge density distribution of the orbital of the excess-electron state that appears in the band gap. The red region in the figure represents an isosurface with a charge density of 0.01\AA^{-3} . The excess electron is localized to one Ti atom, and occupies the Ti d_{zx} orbital. A careful observation of the atomic structure near the excess-electron localized Ti atom suggests that the O atom adjacent to the Ti atom is slightly displaced and lattice distortion occurs locally [Fig. 1(c)]. The small displacements of each O atom are 0.066\AA for the O1 and O2 atoms, 0.026\AA for the O3 and O4 atoms, and 0.067\AA for the O5 and O6 atoms, as shown in Fig. 1(b). This anisotropy corresponds to the anisotropy of the d_{zx} orbital occupied by the excess-electron polaron. Since this local lattice distortion is a typical feature of a polaron [14,29], the excess electron forms a polaronic state in SrTiO₃. Actually, in the previous first-principles calculations for a Nb-doped SrTiO₃ system, an excess electron introduced by a Nb impurity was observed to form a polaronic state in SrTiO₃ [29], which is in good agreement with the polaron formation in our calculations.

B. Evaluation of vortex polarization characteristics of excess-electron polaron

To study the ferroelectric properties induced by excess-electron polarons, we evaluate the local polarization for each local unit cell. Details of the evaluation method are given in the Supplemental Material. Figure 2 shows the spatial distribution of local polarizations in the AFD phase SrTiO₃ in the absence and presence of the excess-electron polaron. When the electron polaron does not exist, the clockwise and counterclockwise microvortex polarizations of the same magnitude are arranged alternately due to the AFD rotational displacement as explained in Supplemental Material and represented in Supplemental Fig. S4. On the other hand, when the electron polaron forms, the arrangement of local polarizations is disturbed around the polaron formation site, and the vortex

polarization on the polaron site is distinguished. Evidently, this change is induced by the formation of the polaron. It is to be noted that such change in polarization arrangement only takes place at the proximity of the polaron formation site, while the arrangement of the remained local polarization is almost the same as that in the absence of the polaron.

To quantitatively characterize the vortex polarizations, the toroidal moment \mathbf{G} is used as a physical quantity [10–12], and is given by the following equation [10]:

$$\mathbf{G} = \frac{1}{2N} \sum_k \mathbf{r}_k \times \mathbf{P}_k \quad (1)$$

where \mathbf{r}_k is the position vector of the k -th local unit cell, \mathbf{P}_k is the local spontaneous polarization at position \mathbf{r}_k , and N is the number of local unit cells contained in the simulation cell. The sum is taken over all unit cells in the analysis cell. In the absence of polaron, the toroidal moment of the system was estimated to be $\mathbf{G}_{\text{perfect}} = (0.00, 0.00, 0.00)\mu\text{C}\text{\AA}/\text{cm}^2$. This result indicates that the AFD phase SrTiO₃ has no macroscopic (net) toroidal moment and does not show ferrotoroidicity in the absence of excess-electron polaron, even though micro-vortex polarizations exist. In other words, the AFD displacement is just a structural displacement that does not contribute to the development of macroscopic (net) polarization or toroidal moment. This result is identical to the recognition of the AFD phase in previous research [31,32]. On the other hand, when the excess-electron polaron is present, a *nonzero* toroidal moment $\mathbf{G}_{\text{polaron}} = (0.00, 0.00, 0.11)\mu\text{C}\text{\AA}/\text{cm}^2$ appears. Therefore, the excess-electron polaron obviously induces a spontaneous toroidal moment.

In order to examine the generation of the toroidal moment by the excess-electron polaron in detail, the difference between the local polarization $\mathbf{P}_{\text{polaron}}$ in the presence of the excess-electron polaron and the local polarization $\mathbf{P}_{\text{perfect}}$ in the absence of the excess electron is evaluated as

$$\Delta\mathbf{P} = \mathbf{P}_{\text{polaron}} - \mathbf{P}_{\text{perfect}}, \quad (2)$$

where $\Delta\mathbf{P}$ indicates the polarization induced by the formation of the excess-electron polaron. Figure 3 illustrates the distribution of $\Delta\mathbf{P}$. The appearance region of $\Delta\mathbf{P}$ is approximately three unit lattices around polaron in the x and z directions and approximately one unit-lattice in the y direction. A closer look at the polarization on the x - y plane reveals a polarization pointing in a direction slightly deviated from the Ti atom in which the polaron is formed [Figs. 3(b) and 3(c)]. Based on this feature, we decompose the component of $\Delta\mathbf{P}$ in the radial direction and the azimuthal direction centered on the polaron formation site. While the radial component does not contribute to the toroidal moment [Fig. 3(d)], the azimuthal component can be a primary source of the toroidal moment [Fig. 3(e)]. Therefore, the azimuthal polarization induced by the formation of polaron should be considered to be the origin of toroidal moment. Note that, since the sum of $\Delta\mathbf{P}$ is 0, the formation of the polaron does not induce any net (macroscopic) polarization.

Next, we discuss the mechanism of the appearance of the local polarization and toroidal moment via the polaron formation. Polarization is defined as the electric dipole moment per unit volume, which corresponds to the spontaneous

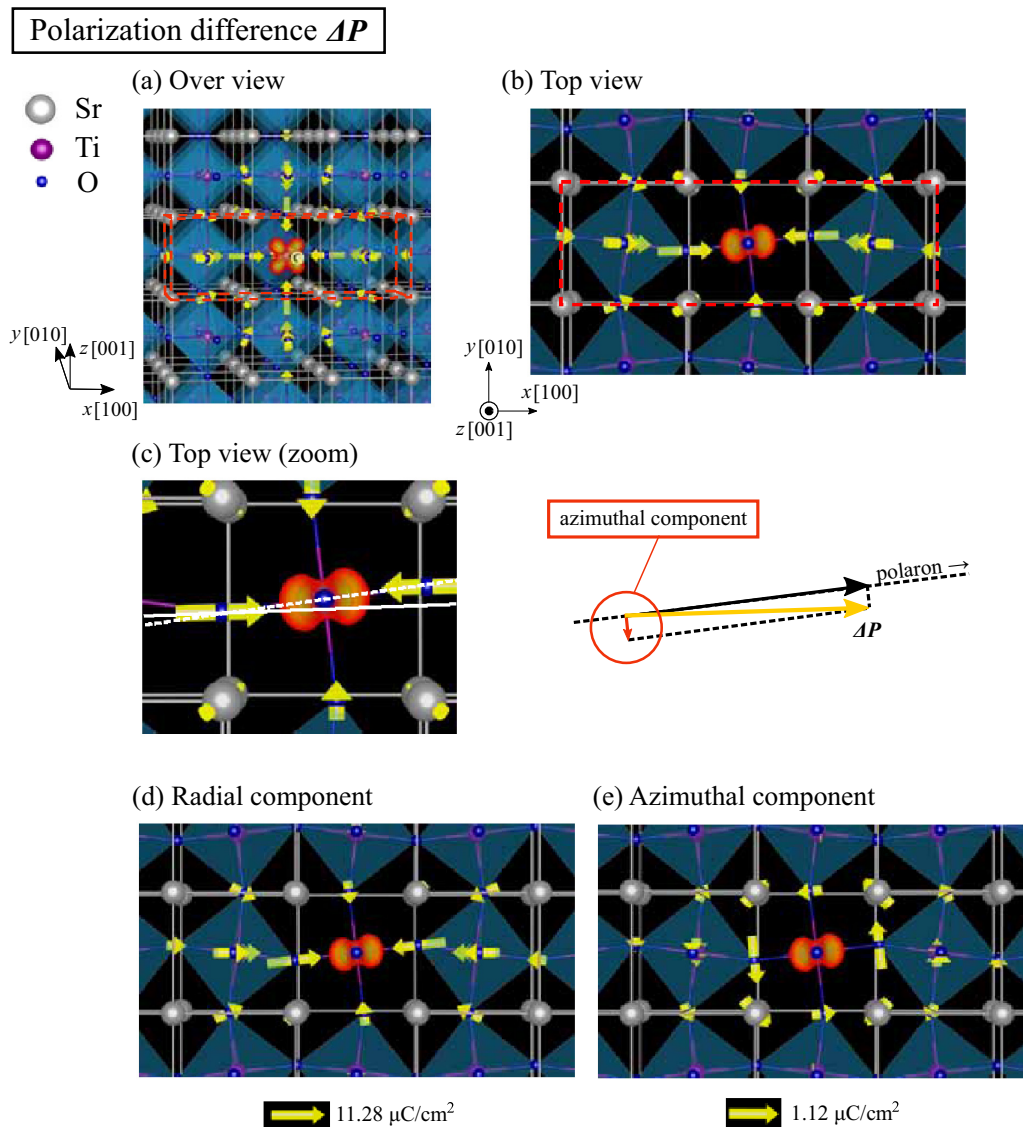


FIG. 3. The polarization induced by the formation of excess-electron polaron in SrTiO_3 . The yellow arrows indicate the difference of local polarization ΔP between SrTiO_3 with and without the polaron. The orange area represents the isosurface of polaron charge densities of $0.01e/\text{\AA}^3$. (a) Overview, (b) top view, (c) top view (zoom), (d) radial component, and (e) azimuthal component.

relative displacement of positive and negative ions in ionic crystals. Thus, we now look at the displacement of each atom induced by the excess-electron polaron, as shown in Fig. 1(c). O atoms nearest to the Ti atom where the polaron is formed exhibit relatively large displacement. The anisotropy of the O-displacement pattern corresponds to the anisotropy of d_{zx} orbital occupied by the localized excess-electron polaron. Moreover, almost no significant displacement is observed in other atoms. Since the O atom is an anion having a negative charge, when the excess-electron polaron is formed on the Ti atom, the negative charge of the polaron and the negative charge of the O atom cause electric repulsion. Thus, the repulsion works to displace each O atom [Fig. 1(c)]. The polarization shown in Fig. 3 thus appears due to this displacement. In addition, the polarization of the O atoms, O1–O4, with AFD displacement obtains components in the direction perpendicular to the components originally possessed by this displacement. Due to the contribution of this

newly obtained component, the azimuthal component of lattice displacement becomes smaller than the original AFD displacement, which weakens the clockwise character of the local polarization vortex of the polaron formation compared with the absence of the excess-electron polaron site, and thus induces counterclockwise polarization vortex in total (Fig. 4). In addition, the atomic displacement induced by the polaron is highly localized at the polaron formation site (only one or two lattices), while there is no such displacement in other sites. This means that the excess-electron polaron carries a highly localized (lattice size) polarization vortex and resulting toroidal moment (Fig. 4). In other words, a spontaneous toroidal moment appears when the polaron locally breaks the symmetry of the local polarization distribution. In addition, the symmetry breaking of this local polarization distribution is caused by the AFD displacement of the AFD phase SrTiO_3 and the introduced excess electron forming a polaron and breaking the structural symmetry locally. In fact,

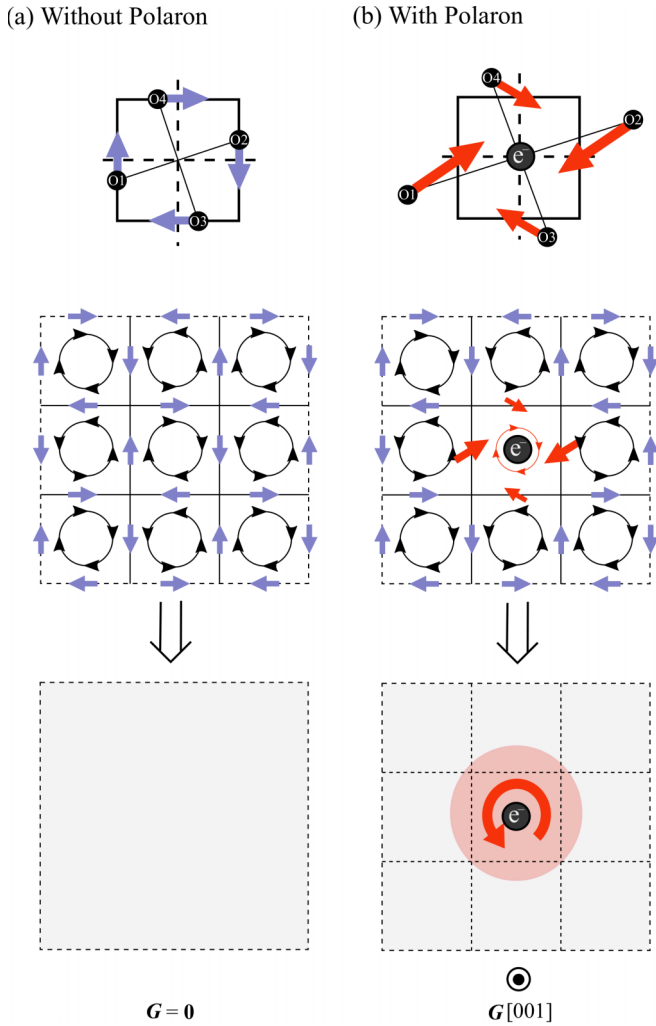


FIG. 4. Schematic illustration of polarization vortices in AFD SrTiO₃ (a) without polaron and (b) with polaron. The blue and red arrows indicate local polarization. The black and red circles indicate the direction of vortices.

the polarization distribution schematically presented in Fig. 4 is well applied to the analysis results given in Fig. 2, and this discussion can explain the analysis results without contradiction. Further, in the paraelectric phase SrTiO₃ without AFD displacement, the excess-electron polaron does not induce a toroidal moment. This also indicates that AFD displacement is necessary for the appearance of the toroidal moment. Based on the above discussion, the appearance of the spontaneous toroidal moment in the AFD phase SrTiO₃ introducing the excess electron can be attributed to the AFD displacement of the tetragonal SrTiO₃ and the local symmetry breaking by the excess-electron polaron.

C. Potential for reversal of toroidal moments via polaron hopping

Figure 5(a) schematically depicts the difference between the directions of toroidal moment depending on the polaron formation site. In the results discussed in the previous section, a toroidal moment appears in the [001] axis direction due

to the excess-electron polaron being formed on the lattice with AFD displacement in the counterclockwise direction. Now, we consider the case where the excess-electron polaron is formed at a site with clockwise AFD displacement, in line with the mechanism discussed in the previous section. We showed that the toroidal moment appears as the excess-electron polaron weakens the vortexlike order that the polaron formation site originally had. Therefore, the direction of the toroidal moment that is developed depends on the rotational direction of the local polarization that originally existed at the polaron formation site. Since the rotational direction of the local polarization corresponds to that of the AFD displacement, the direction of the toroidal moment also depends on the rotation direction of the AFD displacement of the polaron formation site. Thus, when the excess-electron polaron is formed in a lattice with a clockwise AFD displacement, the toroidal moment appears in the [00 $\bar{1}$] direction. These structures relate to mirror symmetry, and both states are energetically equivalent. Therefore, there exist two energetically equivalent toroidal moments in the AFD phase SrTiO₃, which depend on the rotational direction of the AFD displacement at the polaron formation site.

Now, it is generally known that a polaron can move to an adjacent site (hopping) via lattice vibration [14]. The polaron's mobility μ can be obtained by the following equation [33]:

$$\mu = \frac{ea\omega_0}{k_B T} \exp\left(-\frac{E_a}{k_B T}\right). \quad (3)$$

In this equation, e is an elementary charge, a is the movement distance of the polaron to the nearest site, ω_0 is the frequency of the longitudinal optical phonon, k_B is Boltzmann's constant, T is the absolute temperature, E_a is the activation energy required for the polaron to move to the nearest site. E_a can be estimated by the following method [33]. Figure 5(b) shows the activation energy barrier for polaron hopping to the nearest-neighbor site, and we obtain the activation energy barrier of $E_a = 74.40$ meV. Substituting this value and $e = 1.602 \times 10^{-19}$ C, $a = 3.929$ Å, $\omega_0 = 2.40 \times 10^{13}$ s⁻¹ [33], $k_B = 1.381 \times 10^{-23}$ J/K, $T = 300$ K into Eq. (3), we obtain $\mu = 8.05 \times 10^{-2}$ cm²/Vs. It was reported that, for a hole polaron in SrTiO₃, $E_a = 66$ meV and $\mu = 5.09 \times 10^{-3}$ cm²/Vs [33], and the excess-electron polaron in this study is similarly mobile as the hole polaron. On the other hand, the diffusion velocity of oxygen vacancies in oxides was reported to be $10^{-8} - 10^{-6}$ cm²/Vs [34], and the mobility of the excess-electron polaron is several orders of magnitude larger, and the excess-electron polaron has higher mobility than oxygen vacancies. Therefore, it is considered that the excess-electron polaron formed in SrTiO₃ has high mobility and can easily move to the adjacent Ti atom.

Considering the above discussion, it is possible to reverse the direction of the toroidal moment of polaron by moving the excess-electron polaron to an adjacent site. In other words, the excess-electron polaron in the AFD phase SrTiO₃ can invert the toroidal moment by hopping and has a "ferrotoroidic" property. Therefore, the excess-electron polaron can be regarded as an atomic scale ferrotoroidal material.

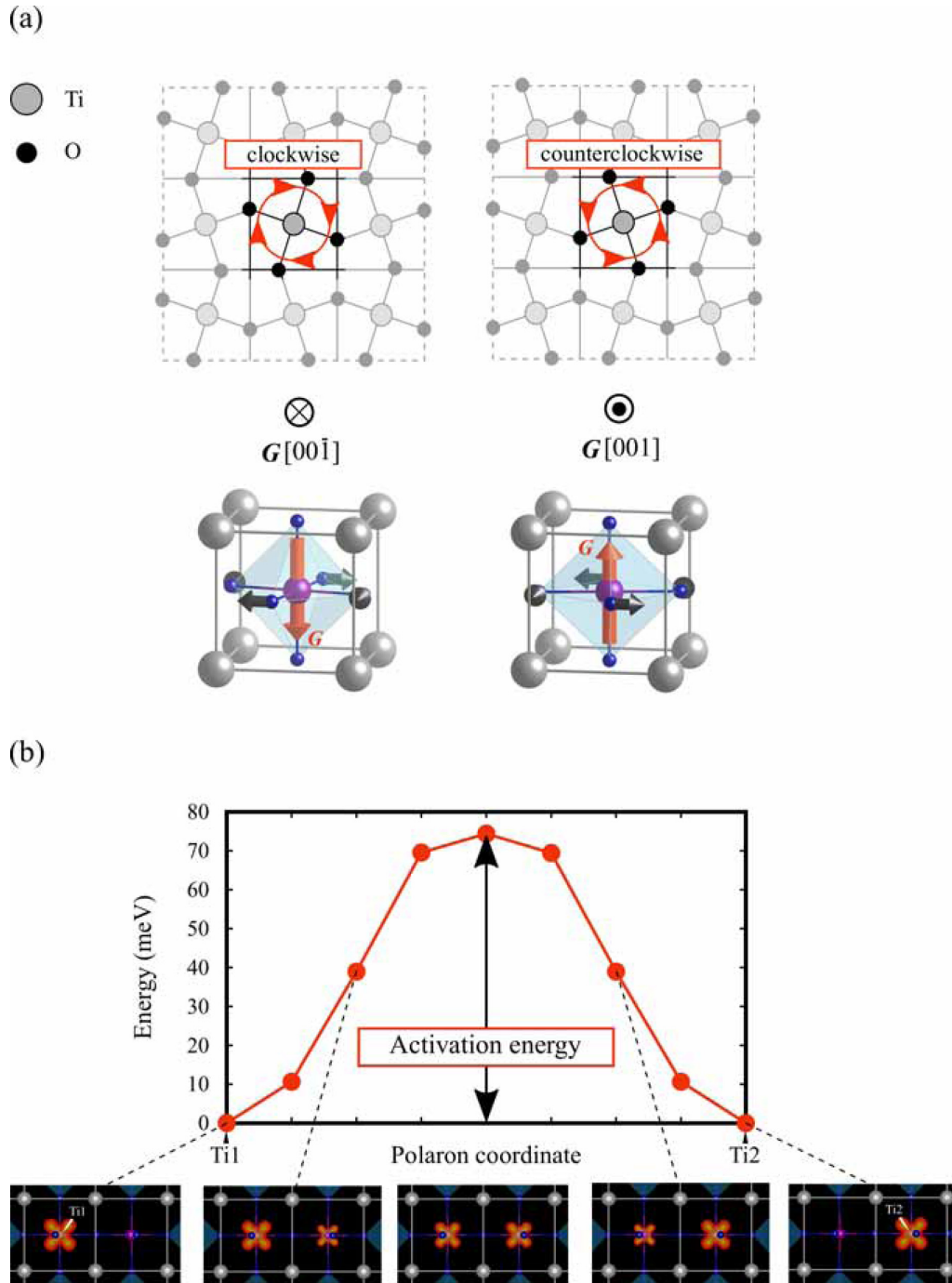


FIG. 5. (a) Schematic illustration of toroidal moment \mathbf{G} induced by polaron in SrTiO_3 . The direction of \mathbf{G} corresponds to the direction of local AFD rotation at the site where the polaron is formed. (b) Energy barrier for polaronic migration in SrTiO_3 from a site with clockwise AFD to the neighboring site with counterclockwise AFD rotation.

D. Multiferroic nature of polarons

While SrTiO_3 is originally a nonmagnetic material, $1 \mu_B$ of magnetism appears in it when the excess-electron polaron exists in SrTiO_3 . Figure 6(a) shows the magnetic density distribution when the excess-electron polaron forms in AFD SrTiO_3 . The magnetic moment is localized to the Ti atom where the excess-electron polaron is formed. Thus, the excess-electron polaron is responsible for the development of magnetism, and behaves as a spin (magnetic) polaron [35].

To discuss the magnetocrystalline anisotropy, the direction of the magnetic moment induced by polaron is evaluated in this part. The component (m_x, m_y, m_z) of the magnetic moment is determined by the following equation, and the total energy for that component is calculated:

$$m_x = \sin \theta \cos \phi, \quad (4)$$

$$m_y = \sin \theta \sin \phi, \quad (5)$$

$$m_z = \cos \theta, \quad (6)$$

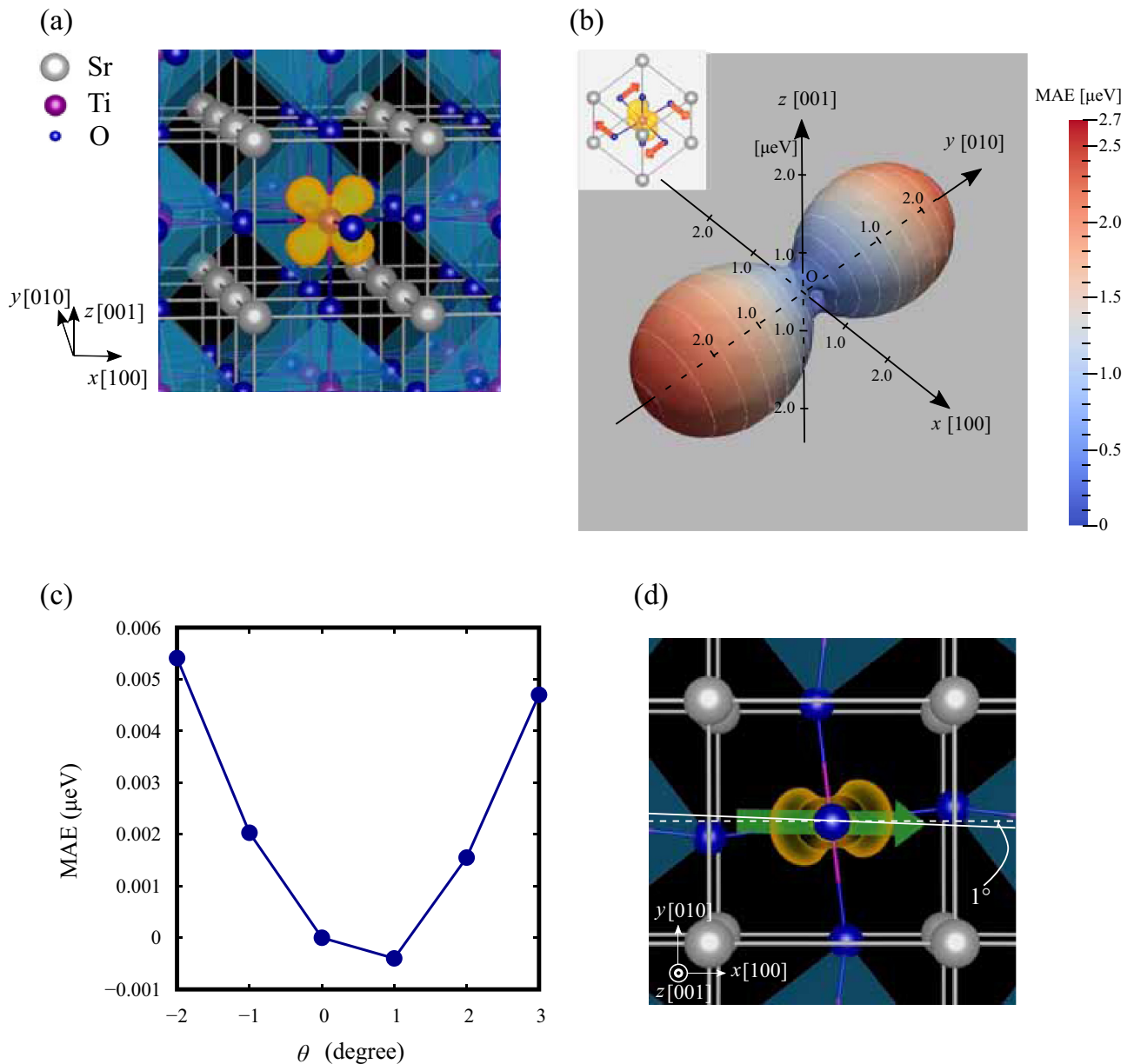


FIG. 6. (a) Magnetic spin-density distribution of the excess-electron polaron in SrTiO₃. The yellow area represents the iso-surface of spin-densities of $0.05 \mu_B/\text{\AA}^3$. (b) Magnetocrystalline anisotropy energy (MAE) surface of excess-electron polaron. The white lines represent the contour lines at every $0.25 \mu\text{eV}$. (c) MAE of around the [100] direction. (d) The direction of magnetic moment of the excess-electron polaron.

where θ is the angle between the magnetic moment and the [001] direction, and φ is the angle between the magnetic moment mapping on the (001) plane and the [100] direction. The values of energy are calculated by changing θ and φ by 10° , respectively. Using this total energy, we calculate the total energy difference defined by the following:

$$\Delta E(m_x, m_y, m_z) = E(m_x, m_y, m_z) - E(1, 0, 0). \quad (7)$$

Here, $E(m_x, m_y, m_z)$ is the total energy when the component of magnetic moment is (m_x, m_y, m_z) . The total energy difference $\Delta E(m_x, m_y, m_z)$ is the magnetocrystalline anisotropic energy (MAE), which indicates energy dependence on the direction of the magnetic moment with respect to the crystal orientation. Figure 6(b) depicts the MAE landscape of the

excess-electron polaron. Note that, to obtain the accurate MAE landscape, the energy convergence criterion in the MAE calculations was set to be strict (i.e., $10 \times 10^{-10} \text{eV}$). The difference between the maximum and minimum MAE, i.e., the energy difference between the cases in which magnetic moment points at the hard and easy axes, is $2.7 \mu\text{eV}$. This is the same order as the value $1.4 \mu\text{eV}/\text{atom}$ [36] of Fe(bcc), which is a general ferromagnetic material. In Fig. 6(b), the MAE is high near the y axis ([010] axis) and is low near the x - z plane. Here, $\Delta E(0, 0, 1) = 0.19 \mu\text{eV}$, and the energy is lower for $(m_x, m_y, m_z) = (1, 0, 0)$ although it is nonzero. Therefore, MAE is minimized when $(m_x, m_y, m_z) = (1, 0, 0)$ [or equivalent $(m_x, m_y, m_z) = (-1, 0, 0)$]. Here, in order to examine the direction of the most stable magnetic moment

in more detail, MAE was studied with $\varphi = 90^\circ$ and θ varied from -2° to 3° in 1° steps [Fig. 6(c)]. As a result, the energy is minimized when $\vartheta = 1^\circ$. Therefore, the most stable direction of the magnetic moment is a direction that is deviated by 1° from the [100] axis. This asymmetry is due to the asymmetry of the crystal structure of AFD phase SrTiO₃. The direction of displacement is opposite to the rotational direction of AFD displacement. From above, the magnetic moment induced by the excess-electron polaron is observed to have crystal magnetic anisotropy, and the magnetic moment is deviated from the [100] axis by 1° in the direction opposite to the rotational direction of the AFD displacement [Fig. 6(d)].

E. Possible magnetoelectric control of toroidal moment of polarons

In general, materials that simultaneously exhibit two different ferroic order parameters, such as ferromagnetism and ferroelectricity, are called as multiferroics [37,38]. As shown above, the excess-electron polaron simultaneously shows two ferroic properties, ferrotoroidity and magnetism. Further, the appearance region of that ferrotoroidity is approximately one unit lattice around the polaron formation site, and magnetism is localized to one Ti atom. Therefore, the excess-electron polaron in AFD SrTiO₃ can be regarded as an atomic-scale multiferroic or a “multiferroic polaron,” a class of functional polaron family such as spin (magnetic) polarons and piezopolarons [35]. In general, the polarization and magnetic moment in multiferroics do not exist independently, and besides the magnetic moment, the polarization also responds to an external magnetic field, and the polarization and the magnetic moment respond to the external electric field [Magnetoelectric (ME) effect]. In the following passage, we briefly discuss the possibility of reverse control of the toroidal moment using the ME effect, if it exists.

Figure 7 schematically shows the combination of the toroidal moment and the direction of the magnetic moment when the excess-electron polaron is formed in the AFD phase SrTiO₃. Since there are two directions of rotation of AFD displacement, the orbital occupied by the polaron, and the direction of the most stable magnetic moment, there are eight possible states in total. Let us consider an example by applying a uniform external magnetic field to the state of Fig. 7(a). At this time, it is energetically stable that the direction of the magnetic moment is directed towards the direction of the external magnetic field. Since the excess-electron polaron can easily move to the adjacent site, the polaron hops to it due to the external magnetic field and transitions to another state where the direction of the magnetic moment, which becomes energetically stable, can be realized. Therefore, if the direction of the external magnetic field is the same as that of the magnetic moment in the state of Fig. 7(g), the state changes from Fig. 7(a) to 7(g), and the direction of the toroidal moment is reversed. There is a possibility that the inversion of the toroidal moment can be controlled by the uniform external magnetic field. Currently, since the polarization responds to the static magnetic field, the excess-electron polaron has an ME effect. The toroidal moment can be reversed via this ME effect. Here, the inversion control of the conventional toroidal moment has been proposed theoretically based on the curled

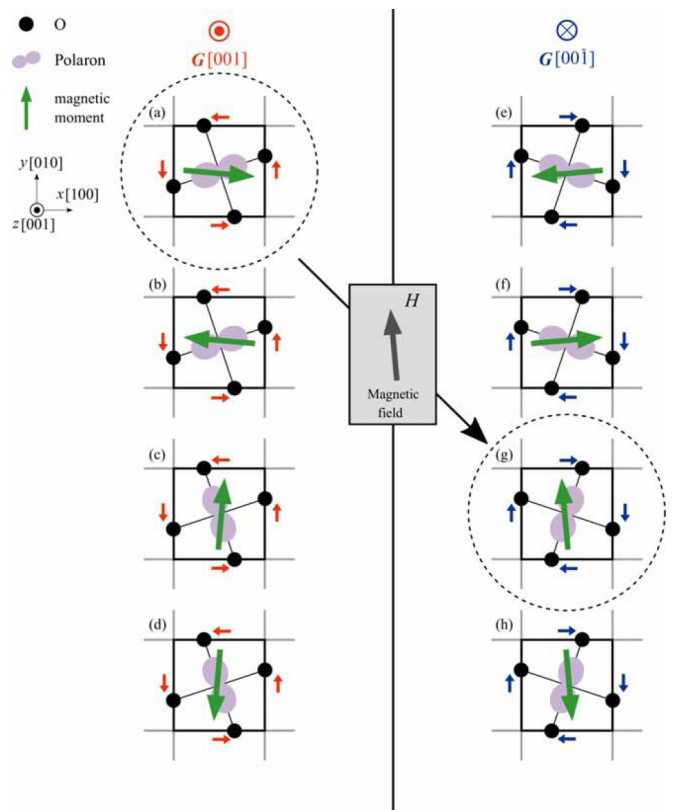


FIG. 7. Schematic illustration of the possible magnetic moment directions of the polaron with positive and negative toroidal moments.

(vortex) electric field formed by the time-varying magnetic field derived from the Maxwell equation $\nabla \times \mathbf{E} = -\partial \mathbf{B} / \partial t$ (\mathbf{E} , \mathbf{B} , and t are the electric field, the magnetic field, and the time, respectively) [10,39], but is considered to be difficult to apply. Therefore, the inversion of the toroidal moment by the ME effect described in this section is different from the conventional method in that it can be realized by a uniform magnetic field. From the above, it is possible that the ferrotoroidicity induced by the excess-electron polaron in the AFD phase SrTiO₃ can be controlled with a uniform magnetic field unlike in the past due to the ME effect of the excess-electron polaron as multiferroics. Note that, a more quantitative aspect on how large magnetic field is required to switch the magnetic moment and polarization of the excess-electron polaron will be discussed in a future work.

It is also interesting to discuss what happens when many excess electrons are introduced into the system (i.e., high carrier densities). In case of the excess electrons, the bipolaron state was not obtained while the two isolated polarons was obtained instead. Different from the hole polaron, which forms a bipolaronlike state [33], the excess electron is unlikely to form the bipolaronic state. This suggests that, at high carrier densities, the ferrotoroidic polarons are kept isolated and repulsively interact each other, and thus such a system is expected to exhibit a unique phase consisting of many ferrotoroidic ordered particles. The detailed study on many-polaron system remains as a future work.

Our theoretical work thus provides a possible ferrotoroidic particle and ferrotoroidic lattice system via the formation and hopping of excess-electron polarons. Experimental verification is also required for a next step. For example, Setvin *et al.* achieved the direct observation of excess-electron polarons in TiO₂ by a scanning tunneling microscopy (STM) [14]. They experimentally addressed each polaron location and its time evolution (i.e., dynamics of polarons) and showed that the observed polaron behavior is consistent with theoretical results. Using such advanced STM techniques, which can identify the polaron location and apply magnetic field, the magnetic field-driven ferrotoroidic switching via the polaron hopping predicted in this work may be experimentally addressed.

IV. CONCLUSION

Using first-principles density-functional theory calculations, we proposed a strategy to overcome existing limitations and design atomically small ferroelectrics with topological

polarization vortices by engineering excess-electron polarons in this paper. Our first-principles calculations established that the excess-electron polaron formed in AFD SrTiO₃ induced localized ferroelectric polarization with a topological vortex form due to local symmetry breaking, and demonstrated the possibility of an atomic scale “ferrotoroidic” material. We further showed that the electron polaron carried a magnetic moment coupled with ferrotoroidicity, i.e., the magnetoelectric effect. We also discussed a possible way to switch the toroidal moment via the magnetoelectric effect. Our results, thus, reveal an approach to ultimate miniaturization of ferrotoroidic materials and a class of functional polaron families.

ACKNOWLEDGMENT

The authors acknowledge financial support from JSPS KAKENHI (17H03145, 18H05241, and 19K21918).

-
- [1] J. F. Scott, *Science* **315**, 954 (2007).
- [2] A. Gruverman and A. Kholkin, *Rep. Prog. Phys.* **69**, 2443 (2006).
- [3] C. H. Ahn, K. M. Rabe, and J. M. Triscone, *Science* **303**, 488 (2004).
- [4] K. Wasa, Y. Haneda, T. Sato, H. Adachi, and K. Setsune, *Vacuum* **51**, 591 (1998).
- [5] H. Gu, Y. Hu, J. You, Z. Hu, Y. Yuan, and T. Zhang, *J. Appl. Phys.* **101**, 024319 (2007).
- [6] W. Z. Wang, O. K. Varghese, M. Paulose, and C. A. Grimes, *J. Mater. Res.* **19**, 417 (2004).
- [7] T. Shimada, X. Wang, and T. Kitamura, *Acta Mech.* **224**, 1261 (2013).
- [8] L. V. Lich, T. Shimada, K. Nagano, Y. Hongjun, J. Wang, K. Huang, and T. Kitamura, *Acta Mater.* **88**, 147 (2015).
- [9] B. J. Rodriguez, X. S. Gao, L. F. Liu, W. Lee, I. I. Naumov, A. M. Bratkovsky, D. Hesse, and M. Alexe, *Nano Lett.* **9**, 1127 (2009).
- [10] I. I. Naumov, L. Bellaiche, and H. Fu, *Nature (London)* **432**, 737 (2004).
- [11] G. Pilania, S. P. Alpay, and R. Ramprasad, *Phys. Rev. B* **80**, 014113 (2009).
- [12] T. Shimada, X. Wang, S. Tomoda, P. Marton, C. Elsässer, and T. Kitamura, *Phys. Rev. B* **83**, 094121 (2011).
- [13] M. J. Polking, M.-G. Han, A. Yourdkhani, V. Petkov, C. F. Kisielowski, V. V. Volkov, Y. Zhu, G. Caruntu, A. P. Alivisatos, and R. Ramesh, *Nat. Mater.* **11**, 700 (2012).
- [14] M. Setvin, C. Franchini, X. Hao, M. Schmid, A. Janotti, M. Kaltak, C. G. Van de Walle, G. Kresse, and U. Diebold, *Phys. Rev. Lett.* **113**, 086402 (2014).
- [15] A. Q. Jiang, Y. Y. Lin, and T. A. Tang, *J. Appl. Phys.* **102**, 074109 (2007).
- [16] M. Wu, Z. Zhang, and X. C. Zeng, *Appl. Phys. Lett.* **97**, 093109 (2010).
- [17] T. Shimada, T. Ueda, J. Wang, and T. Kitamura, *Phys. Rev. B* **87**, 174111 (2013).
- [18] T. Shimada, T. Xu, Y. Araki, J. Wang, and T. Kitamura, *Nano Lett.* **17**, 2674 (2017).
- [19] T. Shimada, J. Wang, T. Ueda, Y. Uratani, K. Arisue, M. Mrovec, C. Elsässer, and T. Kitamura, *Nano Lett.* **15**, 27 (2015).
- [20] P. Hohenberg and W. Kohn, *Phys. Rev.* **136**, B864 (1964).
- [21] W. Kohn and L. J. Sham, *Phys. Rev.* **140**, A1133 (1965).
- [22] G. Kresse and J. Hafner, *Phys. Rev. B* **47**, 558 (1993).
- [23] G. Kresse and J. Furthmüller, *Phys. Rev. B* **54**, 11169 (1996).
- [24] P. E. Blöchl, *Phys. Rev. B* **50**, 17953 (1994).
- [25] G. Kresse and D. Joubert, *Phys. Rev. B* **59**, 1758 (1999).
- [26] H. J. Monkhorst and J. D. Pack, *Phys. Rev. B* **13**, 5188 (1976).
- [27] G. Makov and M. C. Payne, *Phys. Rev. B* **51**, 4014 (1995).
- [28] J. P. Perdew, K. Burke, and M. Ernzerhof, *Phys. Rev. Lett.* **77**, 3865 (1996).
- [29] X. Hao, Z. Wang, M. Schmid, U. Diebold, and C. Franchini, *Phys. Rev. B* **91**, 085204 (2015).
- [30] See Supplemental Material at <http://link.aps.org/supplemental/10.1103/PhysRevB.101.214101> for simulation models and procedure, calculations of local polarizations, and consideration of AFD rotations, which includes Refs. [40–42].
- [31] H. Unoki and T. Sakudo, *J. Phys. Soc. Jpn.* **23**, 546 (1967).
- [32] G. Shirane and Y. Yamada, *Phys. Rev.* **177**, 858 (1969).
- [33] H. Chen and N. Umezawa, *Phys. Rev. B* **90**, 035202 (2014).
- [34] M. Schie *et al.*, *J. Phys.: Condens. Matter* **24**, 485002 (2012).
- [35] J. T. Devreese, *Polarons, in Encyclopedia of Applied Physics* (Wiley-VCH, New York, 1996).
- [36] A. N. Anisimov, M. Farle, P. Pouloupoulos, W. Platow, K. Baberschke, P. Isberg, R. Wappling, A. M. N. Niklasson, and O. Eriksson, *Phys. Rev. Lett.* **82**, 2390 (1999).
- [37] H. Schmid, *Ferroelectrics* **252**, 41 (2001).
- [38] N. A. Spaldin and M. Fiebig, *Science* **309**, 391 (2005).
- [39] S. Prosandeev, I. Ponomareva, I. Kornev, I. Naumov, and L. Bellaiche, *Phys. Rev. Lett.* **96**, 237601 (2006).
- [40] T. Higuchi, T. Tsukamoto, K. Kobayashi, Y. Ishiwata, M. Fujisawa, T. Yokoya, S. Yamaguchi, and S. Shin, *Phys. Rev. B* **61**, 12860 (2000).
- [41] H. Ohta, K. Sugiura, and K. Koumoto, *Inorg. Chem.* **47**, 8429 (2008).
- [42] T. Shibuya *et al.*, *J. Phys.: Condens. Matter* **24**, 435504 (2012).